Colloids and Surfaces A: Physicochem. Eng. Aspects 411 (2012) 129–139

Contents lists available at SciVerse ScienceDirect

Colloids and Surfaces A: Physicochemical and Engineering Aspects

journal homepage: www.elsevier.com/locate/colsurfa

Microencapsulation of oil droplets using freezing-induced gelatin–acacia complex coacervation

Kyuya Nakagawa*, Hiromistu Nagao

Research Center for Nano-Micro Structure Science and Engineering, University of Hyogo, 2167 Shosha, Himeji City, Hyogo 671-2201, Japan

HIGHLIGHTS

- This is a work on engineering nanoparticles that encapsulate oil droplets.
- A gelatin–acacia complex coacervation was employed for encapsulation technique.
- A freezing process was applied to control the kinetics of a complex coacervation.
- The encapsulation properties could be controlled by the cryoprocessing parameters.
- The release patterns could be tuned without changing the chemical compositions.

GRAPHICAL ABSTRACT

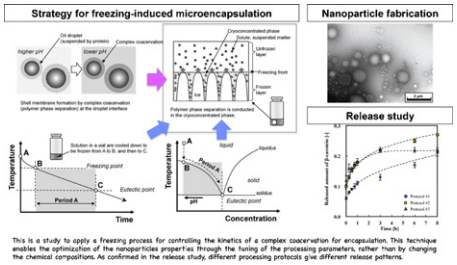

This is a study to apply a freezing process for controlling the kinetics of a complex coacervation for encapsulation. This technique enables the optimization of the nanoparticles properties through the tuning of the processing parameters, rather than by changing the chemical compositions. As confirmed in the release study, different processing protocols give different release patterns.

ARTICLE INFO

Article history:
Received 7 May 2012
Received in revised form 29 June 2012
Accepted 7 July 2012
Available online 17 July 2012

Keywords:
Encapsulation
Nanoparticles
Freezing
Complex coacervation
Gelatin
Acacia

ABSTRACT

A freezing process was applied to control the kinetics of a gelatin–acacia complex coacervation technique for encapsulating emulsified oil droplets. An oil-in-water emulsion was stabilized with a gelatin–acacia solution, and the pH of the solution was adjusted to a selected value with acetic acid. When the pH of the emulsion was adjusted to 4.7, the system was visibly stable at ambient temperature for up to 12 h. Freezing the emulsion caused polymer phase separation (complex coacervation) in the cryoconcentrated phase and resulted in encapsulated oil droplets and the accumulation of a cream layer in the freeze-thawed solution. Observation by transmission electron microscopy clarified the formation of 50–4000 nm core–shell nano-microparticles, the surfaces of which were surrounded by polymeric membranes. The membrane properties of the particulate systems were dependent on the cooling rate that was used during freezing. For example, when an emulsion with a pH of 4.7 was frozen, a cooling rate of −1.0 °C/min maximized the encapsulation yield, whereas a rate of −2.0 °C/min was effective in limiting the release rate of the ingredient (β-carotene) from the oil phase through the shell membrane. The results of this study suggest that the formation of nano-microparticles could be highly associated with the kinetics of freezing, so their resultant properties could be fine-tuned using a freezing operation. This is a potential concept providing a novel strategy for engineering core–shell nanoparticles.

1. Introduction

Encapsulation by complex coacervation is recognized as a potential technique for fabricating nanoparticles with a lipid core. This process could potentially be used for designing nano/microencapsulation systems to realize desirable functions, such as preservability, miscibility, deliverability, and controlled

* Corresponding author. Tel.: +81 792 67 4849; fax: +81 792 67 4849.
E-mail address: nakagawa@eng.u-hyogo.ac.jp (K. Nakagawa).

0927-7757/$ – see front matter © 2012 Elsevier B.V. All rights reserved.
http://dx.doi.org/10.1016/j.colsurfa.2012.07.010

release of the ingredients. Encapsulating oil droplets with coacervate membranes yield core–shell nanoparticles that are of great interest for the pharmaceutical [1–7] and food [8–12] industries. The lipid core enables large amounts of lipophilic substances with low aqueous solubilities to be loaded, and the shell membrane protects the ingredients from unfavorable oxidation and/or controls the diffusion rate of the ingredients through the membrane. This particulate system is a useful vehicle for lipophilic drugs and nutraceuticals, as well as for flavor encapsulation [13,14].

Complex coacervation is a liquid–liquid phase separation phenomenon that occurs when mixing oppositely charged polyelectrolyte solutions. Proteins and polysaccharides are commonly used for complex coacervation for entrapping targeted materials in the concentrated polymer phase [15,16]. In particular, gelatin is widely used in combination with polyanions, such as gum acacia [1–3,5,8,17,18], carboxymethylcellulose [19], sodium dodecyl sulfate [20], chitosan [21,22], agar [23], gellan [24], and pectin [25]. Recent investigations have provided further support for the high potential of complex coacervation for designing functional nano/microencapsulation systems. A challenge is to increase our knowledge of complex coacervation methods and develop standardized protocols for improving the quality of encapsulated products.

The complex coacervation method principally consists of an emulsification step for making an oil-in-water emulsion, a coacervation step for coating the oil droplet surface by adjusting the pH of the solution, and a step for fixating the shell membrane through the gelation of the coacervates or by chemical crosslinking. The technique is a simple and solvent-free process and thus would be highly advantageous for the fabrication of nanoparticles in industry. However, from an engineering perspective, it would be important to ensure a high reproducibility and minimize lot-to-lot variations caused by polymer phase separation [26]. The complex coacervation process is greatly affected by the properties of the polymers, including their molecular weights, concentrations, and ionic charge densities, which are fixed by the formulations [27]. In contrast, other variables, such as the ionic charge balance (controlled by pH adjustment) and the thermal conditions during processing, are fixed by the processing conditions. The development of new approaches for controlling the pH and temperature of coacervation systems would be beneficial.

Motivated by this information, the present work attempted to adopt a freezing process to control the kinetics of complex coacervation. The growth of ice crystals in a solution induces a liquid–solid phase separation, in which the liquid phase is known as the cryoconcentrated (or freeze-concentrated) phase. As schematized in Fig. 1, the freezing front rejects solutes when the velocity is sufficiently low, whereas it engulfs solutes when the velocity is high. As a consequence, freezing leads to the formation of an ice microstructure when the freezing front progresses at a certain velocity [28]. The concentration of solute in the cryoconcentrated phase is controlled by the phase equilibrium (Fig. 1). When the temperature of a freezing solution is fixed, the solute concentration of the cryoconcentrated phase coincidently follows the phase equilibrium. When oppositely charged polymers are freeze-concentrated with a pH control agent (i.e., an acid), a complex coacervation can be induced by controlling the solution temperature. In a eutectic system, the solute concentration of the cryoconcentrated phase can theoretically be variable between that of the original and the eutectic. Freezing enables highly concentrated microspaces to be realized without loading alternative additives. Polymer phase separation is known (based on the problems it causes during industrial pharmaceutical freeze-drying) to be induced in freezing systems [29,30]; thus, it may be useful for fabricating nanoparticles by complex coacervation.

In this work, a gelatin–acacia solution was used to encapsulate oil droplets by complex coacervation induced by freezing. First, coacervate formations from frozen gelatin–acacia solution and gelatin–acacia oil-in-water (o/w) emulsion were assessed. Second, the core–shell structures of the fabricated particles were observed with transmission electron microscopy (TEM). Finally, release tests of a lipophilic ingredient (β-carotene) were conducted with fabricated specimens for studying the shell membrane properties.

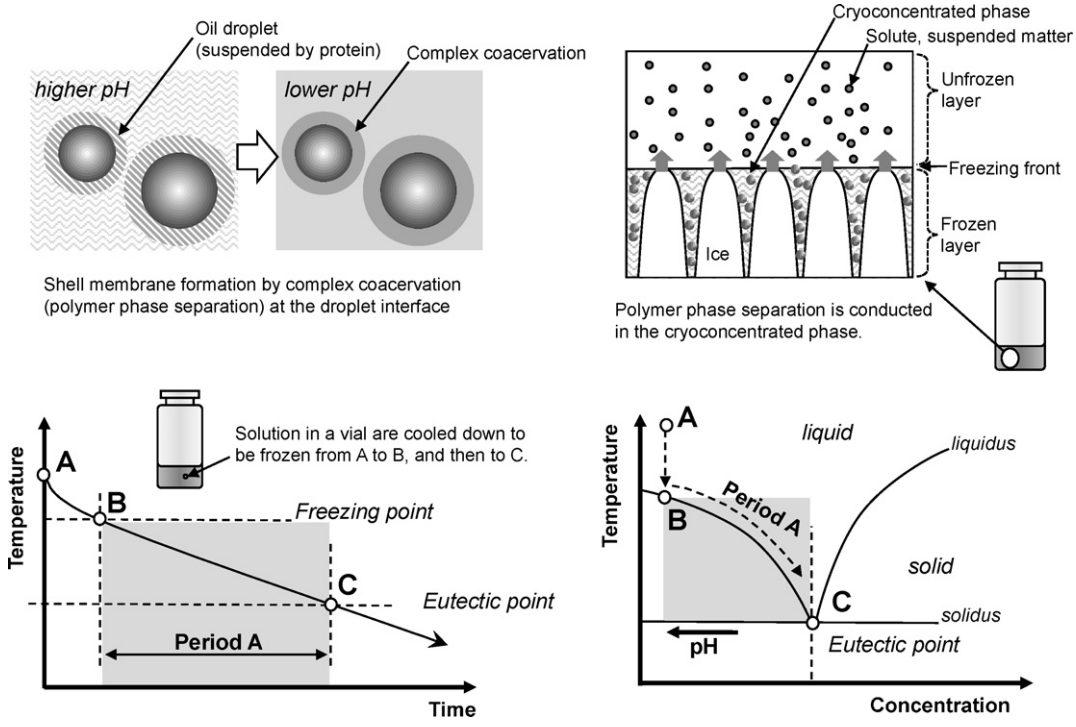

Fig. 1. Particle fabrication by freezing-induced complex coacervation (schematic illustrations).

2. Materials and methods

2.1. Materials

Gelatin (from porcine skin type A, ~300 bloom), acacia gum (analytical grade), and β-carotene (type I) were purchased from Sigma–Aldrich Co. Ltd., Japan. Triolein was supplied by Tokyo Chemical Industry. All the other chemicals used in this work were of analytical grade.

2.2. Nano-microparticle fabrication procedures

A gelatin solution (2%, w/v) was prepared by dissolving gelatin granules in distilled water, with stirring at 60 °C. A 90 mL gelatin solution was mixed with 10 mL of β-carotene solution (1000 ppm of β-carotene dissolved in triolein) and emulsified with a high-speed homogenizer (Clearmix, M-Technique Co. Ltd., Japan) at 18000 rpm for 3 min. Five grams of gum acacia was added to 100 mL of the obtained o/w emulsion with stirring at 60 °C. The pH of the obtained solution, measured using a pH meter (SK-620PH, Sato Keiryoki MFG Co. Ltd., Japan), was 5.60. Acetic acid was carefully added to the gelatin–acacia o/w emulsion until the desired pH levels (4.7, 4.0, and 3.1) were achieved. Each 0.5 mL solution was poured into a vial (2 mL tubing vial with a diameter of 10 mm), and the vials were set on a cooling plate. The cooling plate temperature was controlled by an external coolant circulation system (FP50, Julabo, Germany). The solutions in the vials were frozen using the following 3 freezing protocols:

FR (rapid freezing): the heat exchanger surface was first stabilized at 20 °C. Then, coolant that had been precooled to −40 °C was loaded into the heat exchanger.

FC (constant rate freezing): the heat exchanger surface was first stabilized at 20 °C by the circulated coolant. Then, the coolant was cooled down to −40 °C at −1 °C/min.

FS (constant rate freezing/slow): the heat exchanger surface was first stabilized at 20 °C by the circulated coolant. Then, the coolant was cooled down to −40 °C at −0.25 °C/min.

The mean cooling rates of the solutions during these freezing protocols were measured to be −2.0, −1.1, and −0.26 °C/min for the FR, FC, and FS protocols, respectively.

The obtained frozen samples were subsequently freeze-thawed for observation with TEM or freeze-dried to obtain dried specimens. Freeze-drying was carried out in an evacuated chamber at approximately 10–20 Pa. After the 48 h primary drying stage (temperature of −10 °C), secondary drying was carried out at 25 °C for 3 h. Before the analyses, the freeze-dried specimens were stored in a vacuum desiccator at room temperature, without direct exposure to the sun.

2.3. Viscosity measurement

In order to assess gelling property of the solutions, viscosity was measured under controlled cooling conditions. A rheometer with the concentric cylinder attachment was used for the measurement (AR2000ex, TA Instruments, USA). A 6 mL of the o/w emulsion prepared via the procedure in Section 2.2 was set in the sample space. Temperature was first stabilized at 25 °C and then cooled to 5 °C at −2 °C/min or −1 °C/min, simulating the FR and FC freezing protocols. Viscosity data was collected every 0.5 °C of temperature step at shear rate of 2.0 s^{-1}.

2.4. TEM observation

The freeze-dried specimens were rehydrated with distilled water. A meshed Cu grid was dipped in the solution and dried in a vacuum desiccator overnight. The specimens were then observed using TEM (JEM-2100, JEOL Co. Ltd., Japan). Based on the obtained TEM images, mean particle sizes were estimated by analysis software (ImageJ 1.40 g). At least 400 particle samples were counted from two or three different pictures for each specimen.

2.5. Release test

The release curves of β-carotene were obtained in an ethanol solution. A freeze-dried specimen was crushed into granules, of which 20 mg was put into 1 mL of ethanol and shaken for 1 min until the dried samples were saturated with the solvent. Another 4 mL of ethanol was added to the solution, and from this moment, 20 μL of the solution was sampled periodically for 3 h to detect the release pattern of β-carotene. The β-carotene concentration in each sampled solution was analyzed using an ultraviolet–visible (UV–vis) spectrophotometer (Nanodrop 2000C, Thermo Fisher Scientific Inc., USA). The total mass of β-carotene in each freeze-dried specimen was used to standardize the released amount, so the amount of non-associated (oil off) β-carotene was not subtracted from the value. The total released amount of β-carotene was evaluated with a solution sampled after 24 h.

2.6. Zeta (ζ)-potential measurement

The zeta (ζ)-potentials of the gelatin, acacia, and gelatin o/w emulsions were determined by dynamic light scattering (Zetasizer NanoZS, Malvern Instruments Ltd., Worcestershire, UK). Measurements were carried out at 25 °C in triplicate.

2.7. Turbidity measurement

The turbidity of the gelatin–acacia solution (specially prepared, 0.2% and 0.5% (w/v) of gelatin and acacia, respectively) and gelatin–acacia o/w emulsion (specially prepared via the former method by replacing the gelatin and acacia concentrations with 0.2% and 0.5% (w/v), respectively) were measured by detecting visible light absorption at 750 nm with a spectrometer (QE65000, Ocean Optics Co. Ltd., USA).

2.8. Phase equilibrium data measurement

Phase equilibrium data for the aqueous acetic acid system containing 0.2% (w/v) gelatin and 0.5% (w/v) acacia were generated by differential scanning calorimetry analysis (DSC8500, Perkin-Elmer, USA). The solutions were first cooled to −40 °C and then heated to 60 °C at 10 °C/min. Endothermic peaks were used to obtain solid–liquid phase equilibrium plots.

3. Results and discussions

3.1. ζ-Potential of the solutions

The ζ-potentials of the gelatin solution, gelatin o/w emulsion, and acacia solution were plotted as a function of the pH (Fig. 2). The gelatin (type A) used in the study showed a typical trend of positive values in the measured pH range (1.8–7.0), with increases in the ζ-potential with a decreasing pH. The acacia exhibited an opposite charge to the gelatin solution over the measured pH range; therefore, coacervation could occur at a pH where the charge opposition is wider than a certain level [17]. The plot for the gelatin o/w emulsion was different from that of the gelatin solution. The pH range where the charge opposition was maximized was narrower than that for the gelatin solution.

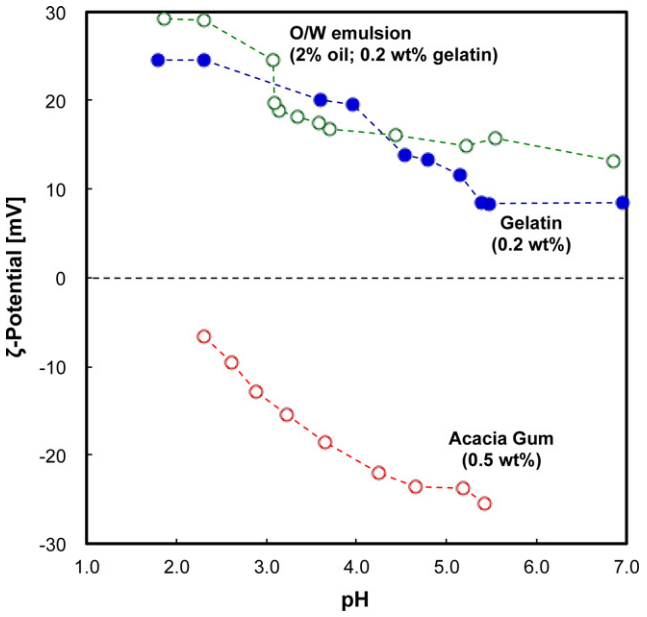

Fig. 2. The pH dependence of the ζ-potential.

3.2. Phase separation of the solutions before and after freezing

The phase separation of the gelatin–acacia solutions is summarized in Fig. 3a. Phase separation could clearly be confirmed in the solutions with pH levels of 3.0 and 4.0, whereas it was not visible in the others. These solutions were frozen in a refrigerator at −40 °C (cooled by air convection) overnight and then thawed at ambient temperature for 3 h. Comparisons of the phase separations of the solutions are presented in Fig. 3b. It is interesting that clear phase separations could be confirmed for all the solutions containing acetic acid, except for one with a pH of 2.0. It was evident that the freezing induced gelatin–acacia complex formation.

Similar analyses were made with gelatin–acacia o/w emulsions. For the unfrozen emulsions, as observed for the gelatin–acacia solutions, apparent phase separations could be confirmed at pH levels between 3.0 and 4.0 (Fig. 4a). Turbid phases appeared in the upper portion owing to creaming of the emulsion. The creaming appeared to be caused by the gelatin–acacia complex coacervation at the interfaces of the oil droplets. It was observed in a separate experiment (data not shown) that spontaneous creaming slowly proceeded in the set of the solutions; visible phase separation was confirmed 1–2 days after the emulsification. As confirmed in Fig. 4b, creaming was confirmed in all the solutions after freezing, where freezing was conducted within 1 h of emulsification. This creaming could be partly due to the complex coacervation. However, for the solution that did not contain acetic acid (pH 5.4), this phase separation could simply be associated with emulsion instability caused by freezing. Freezing provokes a lot of phenomena that affect emulsion stability [31,32]. Based on previous reports, dehydration due to ice crystal formation would enhance the interaction between droplets and cause their coalescence, adsorption of the emulsifier onto the ice crystal surface may reduce the emulsion stability, and freeze concentration of solutes and suspended matters could further affect the emulsion stability. In this study, the authors consider that the addition of acetic acid would lead to emulsion instability due to the complex coacervation of the gelatin–acacia system. A phase diagram of the aqueous acetic acid system containing gelatin

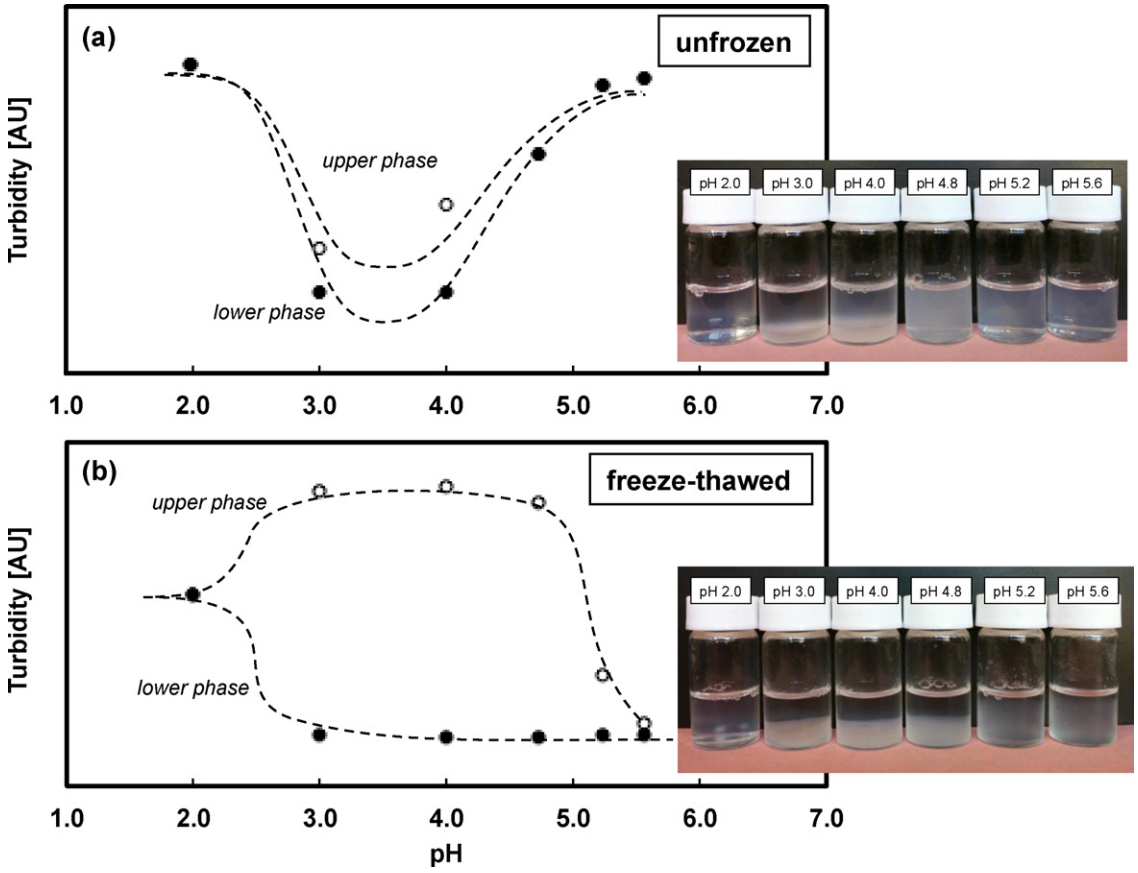

Fig. 3. The pH dependence of the phase separation (gelatin–acacia solution); open circle: upper phase, closed circle: lower phase, (a) unfrozen solution and (b) freeze-thawed solution.

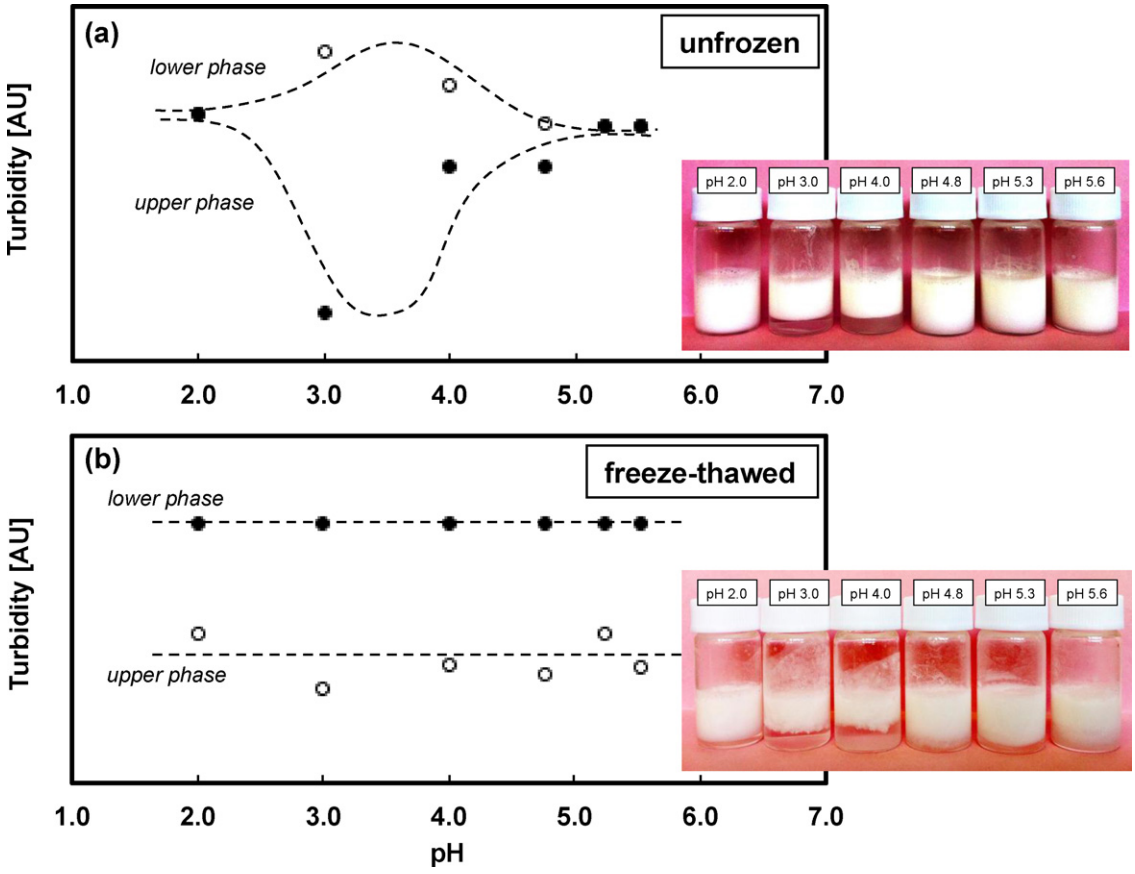

Fig. 4. The pH dependence of the phase separation (gelatin–acacia o/w emulsion); open circle: upper phase, closed circle: lower phase, (a) unfrozen solution, (b) freeze-thawed solution.

and acacia is presented in Fig. 5. The obtained diagram was close to that of the water–acetic acid binary system, suggesting that the contribution of gelatin and acacia to the lowering of the freezing point was not obvious compared with that of acetic acid. The phase diagram showed that the acetic acid concentration in the cryoconcentrated phase reached approximately 58 wt% at the eutectic point. The equilibrium freezing points for the solutions with pH levels of 4.8, 4.0, and 3.0 were −0.03, −0.3, and −3.7 °C, respectively.

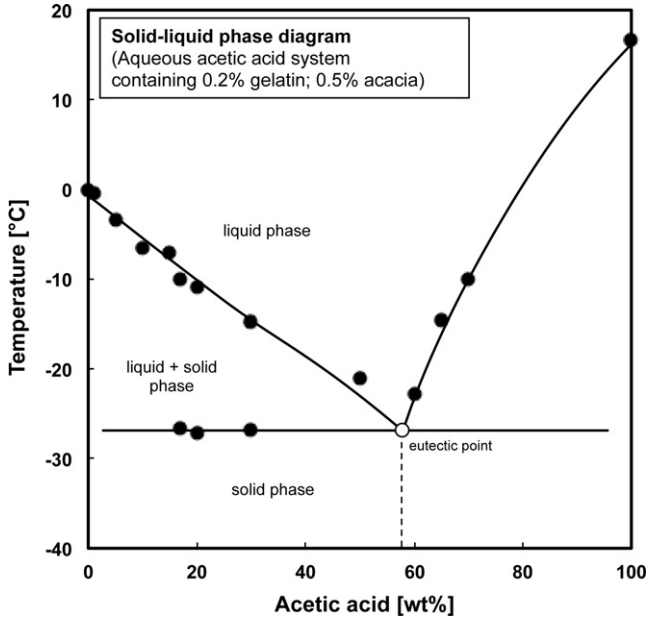

Fig. 5. Phase diagram of the aqueous acetic acid system containing gelatin and acacia.

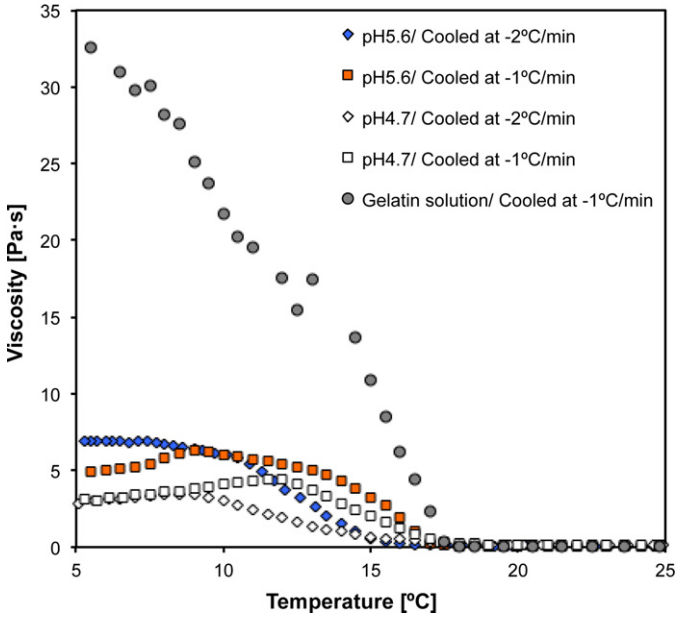

Fig. 6. The viscosity profile of the solution during cooling.

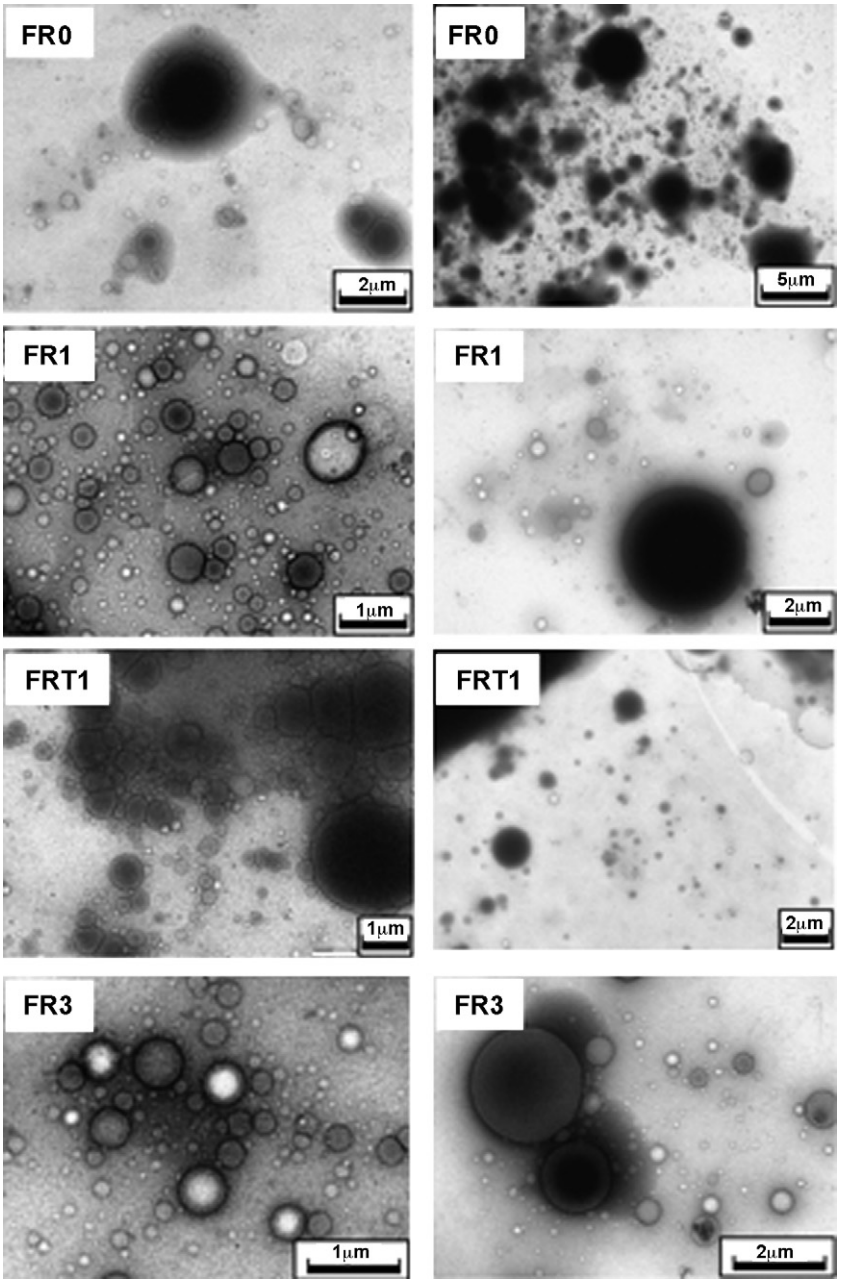

Fig. 7. TEM images of the specimens, FR0, FR1, FRT1, FR3 (the specimen IDs are listed in Table 1).

When the temperature of the freezing solution was −3.7 °C, the pH of the cryoconcentrated phase should coincidently be set to pH 3.0. The cooling rate during freezing must correspond to the rate of pH decrease. Our major interest in this work is to know the influence of this kinetic parameter on the formation of nanoparticles by complex coacervation.

3.3. Viscosity profile during cooling

The gelling characteristics of the present emulsion system upon cooling were analyzed as shown in Fig. 6. When an aqueous gelatin solution (2%, w/v) was cooled at −1 °C/min, the uptake of the viscosity was observed at around 17 °C, and it continued to increase above 35 Pa s until 5 °C. When the emulsions were cooled down, the uptake of the viscosity was also observed at around 17 °C. However the viscosity increase was saturated at around 4–6 Pa s. The uptake rate was slowed by increasing cooling rate and by adding acetic acid. Free gelatin would make segregated gel networks and localized in the solution. This resulted in slight increase of the viscosity. The oil droplets associated with the gelatin and acacia would suspend with the free gels.

3.4. TEM analysis of the prepared nano-microparticles

The observations of the particles fabricated via the procedure shown in Section 2.2 were made with TEM. Figs. 7 and 8, the specimen IDs are listed in Table 1. These analyses confirmed the formation of a shell membrane surrounding a lipid core. The particle sizes varied from approximately 50–4000 nm and were affected by the emulsification and postprocessing conditions (thawing and freeze-drying). The thicknesses of the membranes varied from approximately 10–50 nm, depending on the size of the particles, with thicker membranes for larger particles and vice versa. It is worth noting that nano-microparticles were successfully prepared

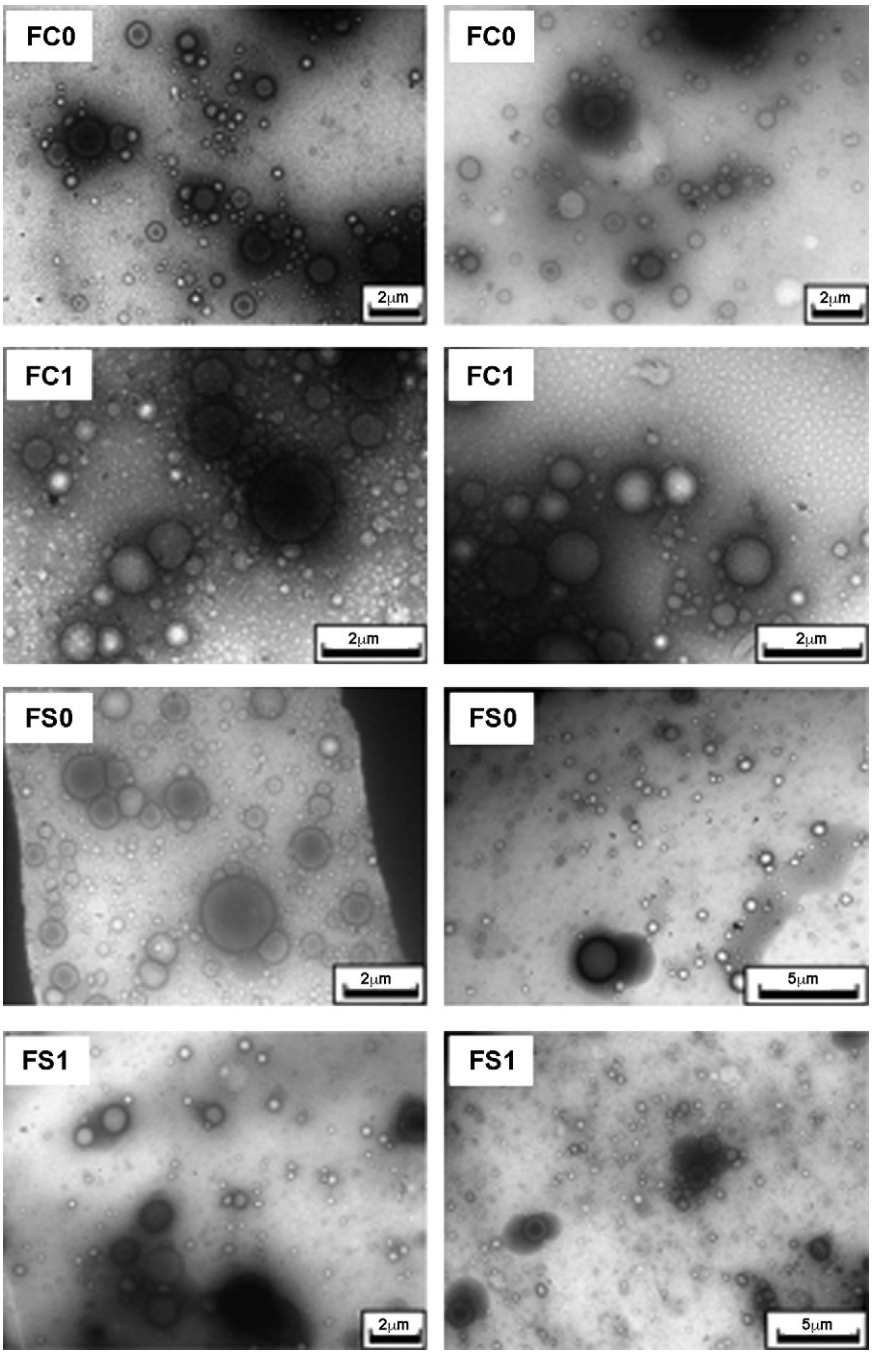

Fig. 8. TEM images of the specimens, FC0, FC1, FS0, FS1 (the specimen IDs are listed in Table 1).

via all the conditions used. The images demonstrated aggregated and well-dispersed particles. Larger particles (approximately 1000–3000 nm) were usually associated with small particles and sometimes appeared in deformed spheres. This trend was often seen in the specimens FR0 and FC0. For the specimens that did not contain acetic acid (FR0, FC0, and FS0), we often found free polymeric matrices that were not associated with nanoparticles. These free polymeric matrices were also confirmed in the other specimen containing acetic acid, although usually very small particles were embedded in the matrices (as was obviously apparent in the image for FC1). FR3 was prepared from a solution with a pH of 3.1; therefore, complex coacervation occurred before the freezing step. The images obtained for FR3 were visibly similar to those from FR1. The mean particle sizes were analyzed from the TEM images as summarized in Fig. 9. It was obvious that the particles prepared with acetic acid were smaller than that prepared without the acid. The mean particle sizes for FR1 and FR3 were 236 and 204 nm, respectively. Whereas, that for FR0 was approximately two times higher, that was, around 427 nm. Further, the different freezing condition yielded different size of particles. When acetic acid was added, slower cooling condition yielded larger particle. This trend was, however, not seen in the specimens not containing acids, so the acid addition evidently contributed to the particle formation via freezing. For FRT1, the specimen prepared by applying rapid freezing and thawing, the formation of a particulate system was observed, as in the freeze-dried specimen (FR1); however, deformed particles were often observed, and the mean particle size (ca 292 nm) was higher than that for FR1. The data suggest that

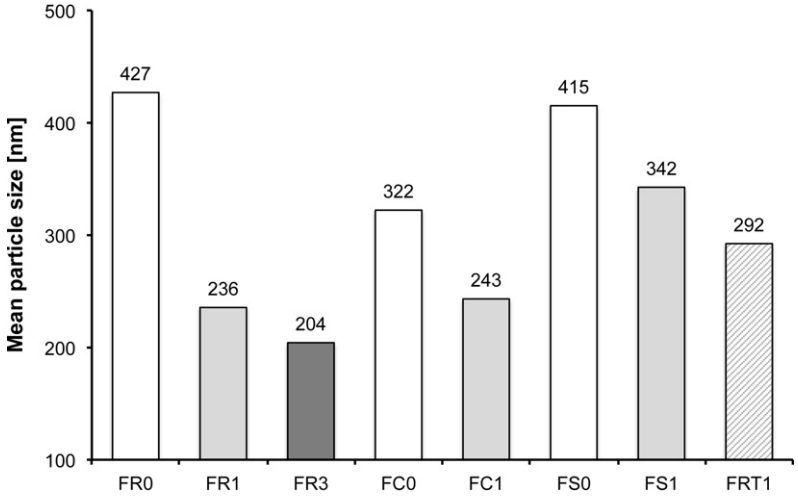

Fig. 9. The mean particle size of the specimens.

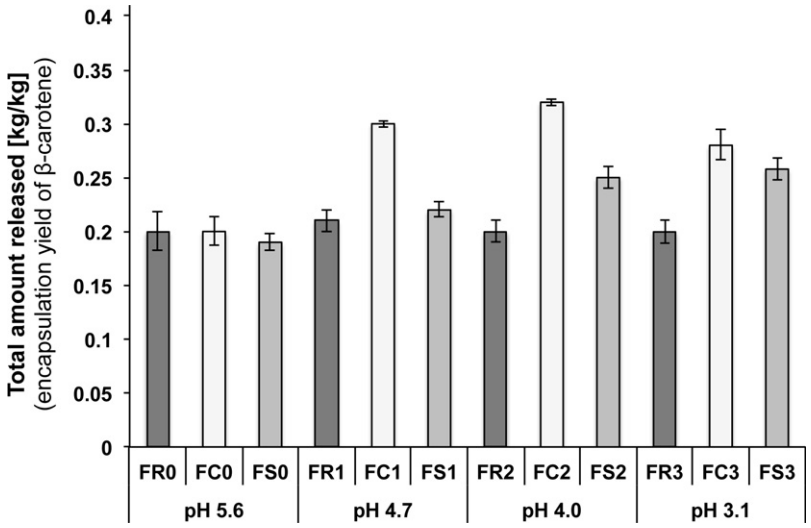

Fig. 10. The total amounts of β-carotene released from the prepared nano-microparticles (the specimen IDs are listed in Table 1).

the appearance of the particles was not permanently fixed during freezing but could change after rehydration.

3.5. Release curves of the prepared nano-microparticles

The release tests were conducted in ethanol solution to assess the encapsulation yields and to clarify the differences in the shell membrane properties. The total amounts of β-carotene released by the different specimens are compared in Fig. 10. Approximately 0.20–0.35 kg/kg of β-carotene was recovered after the encapsulation. These values were standardized to the total β-carotene load in the oil phase, so they included any loss that occurred during emulsification (e.g., degradation or oxidization during mechanical homogenization) and encapsulation (e.g., oil off). It was apparent that the freezing protocols did not affect the encapsulation yields of specimens FR0, FC0, and FS0, which did not contain acetic acid. When the pH levels of the original solutions were adjusted to 4.7 or 4.0, the freezing protocols clearly influenced the total amounts of β-carotene released. The protocol FC (i.e., that with a mean cooling rate of −1.1 °C/min) was found to be favorable in terms of maximizing the encapsulation yields. The protocol FR (−2.0 °C/min) gave almost constant yield values of approximately 0.2 kg/kg, whereas FS (−0.26 °C/min) gave slightly higher yields for the solution with a pH of 4.0. The specimens prepared from the solution with a pH of 3.1 exhibited similar encapsulation yields to those prepared from the solutions with pH levels of 4.7 and 4.0. As discussed earlier, in those solutions, the shell membranes (i.e., complex coacervation) of the particles could be formed owing to adjustments in the acidity. Therefore, a contribution of freezing was mainly to cause damage to the preexisting nano-micorparticles penetrated by the ice crystals.

Table 1
Specimen IDs.

ID	pH adjustment	Freezing protocol	Preparation method
FR0	No additive (pH 5.6)	FR	Freeze-drying
FR1	pH 4.7	FR	Freeze-drying
FR2	pH 4.0	FR	Freeze-drying
FRT1	pH 4.7	FR	Freeze–thawing
FR3	pH 3.1	FR	Freeze-drying
FC0	No additive (pH 5.6)	FC	Freeze-drying
FC1	pH 4.7	FC	Freeze-drying
FC2	pH 4.0	FC	Freeze-drying
FC3	pH 3.1	FC	Freeze-drying
FS0	No additive (pH 5.6)	FS	Freeze-drying
FS1	pH 4.7	FS	Freeze-drying
FS2	pH 4.0	FS	Freeze-drying
FS3	pH 3.1	FS	Freeze-drying

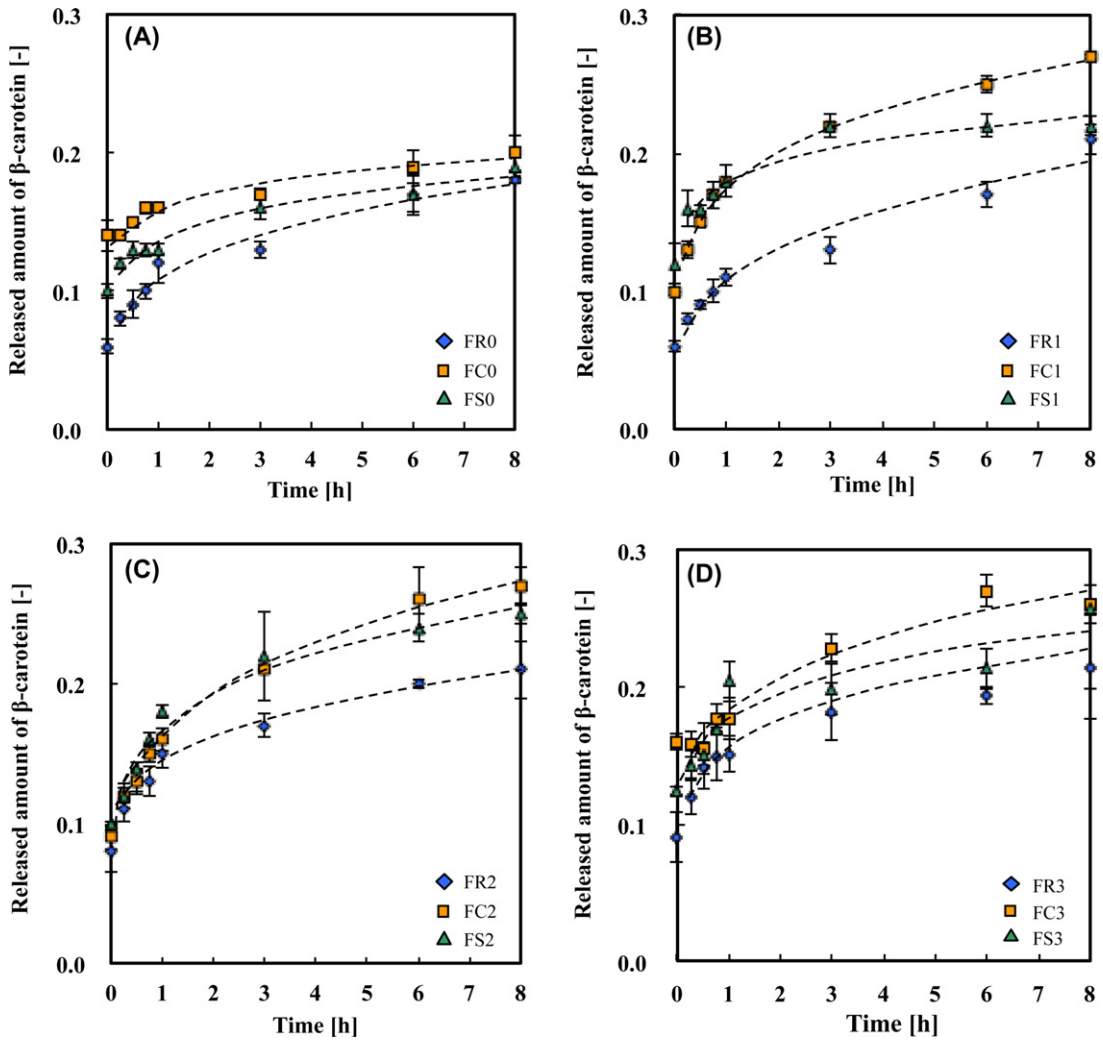

Fig. 11. The release profiles of β-carotene from the prepared nano-microparticles.

As reported in previous studies [33–35], rapid freezing was advantageous for keeping nanoparticle stability, and it was evident that the results of the present study also followed this trend.

The β-carotene release curves for the different freezing protocols were compared in Fig. 11. These plots were fitted by the following equation:

$$Q_{\text{release}} = Q_{\infty} k t^{n} \quad (1)$$

where, Q_{release} is the released amount of β-carotene, Q_{∞} is the total released amount (the value was taken from Fig. 10), k is the kinetic constant and n is the diffusional release exponent [36]. The kinetic constant indicates the rate of release, and the exponent suggests the type of mass transfer. The exponent value becomes 0.5 when the release kinetics is controlled by the Fickian diffusion. This value deviates from 0.5 in case of anomalous diffusion, due to polymer swelling, particle shape variance, particle size distribution etc. [37]. The dotted lines in the figure represent the obtained fitting curves. The obtained parameters were listed in Table 2. Judging from the exponent values, the present release systems were clearly controlled by non-Fickian diffusion, as confirmed in the other literature [38]. Although the encapsulation yields for specimens FR0, FC0, and FS0 were not largely different, their release curves were fairly different from each other (Fig. 11a). The freezing protocol FC caused an initial burst of release of the encapsulated β-carotene (i.e. larger k and smaller n), whereas the protocol FS and FR were slightly successful in terms of reducing this initial burst (i.e. faster cooling rate lead smaller k and larger n). When nano-microparticles were fabricated from the solution with a pH of 4.7, the release patterns differed obviously (FR1, FC1, and FS1). The release curves for FC1 and FS1 overlapped for the first 3 h. In addition, the release for FS1 almost terminated, whereas that for FC1 lasted for more than 8 h until the amount of released β-carotene reached 0.3 kg/kg. The pattern of release from FC1 showed a smaller initial burst and was much slower than those observed for FC1 and

Table 2
Parameters used to fit β-carotene release curves.

ID	Condition	Kinetic constant, k	Exponent, n	Correlation coefficient, R
FR0	pH 5.6 (in Fig. 11A)	0.55	0.24	0.98
FC0		0.80	0.10	0.98
FS0		0.73	0.13	0.97
FR1	pH 4.7 (in Fig. 11B)	0.51	0.28	0.97
FC1		0.59	0.20	0.99
FS1		0.80	0.20	0.99
FR2	pH 4.0 (in Fig. 11C)	0.72	0.18	0.99
FC2		0.50	0.25	0.99
FS2		0.67	0.20	0.99
FR3	pH 3.1 (in Fig. 11D)	0.78	0.18	0.99
FC3		0.68	0.15	0.92
FS3		0.65	0.19	0.97

FS1. For this specimen, the release lasted for approximately 8 h until the amount of released β-carotene reached 0.22 kg/kg. The total released amount for FS1 and FR1 were similar, although they showed quite different release profiles with clearly different diffusional release exponent values. As increasing the cooling rate, n value increased, suggesting the difference in the membrane properties. However, the dependency on the freezing protocols was not obvious in the specimens produced from solutions that were adjusted to pH 4.0 (FR2, FC2, and FS2). The kinetic parameters did not highly dependent on the freezing protocols. The release patterns for the specimens FC3 and FS3 (produced from solutions with a pH of 3.1) were burst types, whereas that for FR3 was quite similar to that for FR2 as also known from the kinetic parameter values. For specimens FR3, FC3, and FS3, as noted earlier, the particle formation process could almost have terminated before freezing because of the adjustments in the acidity. On the other hand, that for FR2, FC2, and FS2 would be partly achieved before freezing and partly fixed during freezing.

The results described earlier suggest that the formation of the nano-microparticles was highly associated with the kinetics of freezing. A freezing protocol fixes the temperature history during freezing and, as a consequence, fixes the concentration history in the cryoconcentrated phase. When a system (pH 4.8) was frozen by the FR protocol (−2.0 °C/min), it took approximately 1.8 min for the temperature to change from −0.03 °C to −3.7 °C. These temperatures correspond to the equilibrium freezing temperatures of the solutions with pH levels of 4.8 and 3.0, respectively. It has been reported that the kinetics of protein–polysaccharide complex coacervation occurred with a time scale of a few minutes at ambient temperature [39]. The kinetics is dependent on the ratio of the protein and polysaccharide, as well as the pH and temperature. In a freezing system, the kinetics of a complex coacervation should differ from those under an ambient condition owing to its low temperature and the freeze-concentration effect of the polymers. We, however, do not have enough information to estimate this. Nonetheless, in the system frozen using the FR protocol, the duration required for the pH to shift from 4.8 to 3.0 is estimated to be 1.8 min. This estimation increases to 3.3 min with the FC protocol and 14 min with the FS protocol. These durations seem likely to have an impact on the kinetics of the polymer phase separation and the subsequent shell membrane formation at the interface of the oil droplets. Shell membranes formed via different kinetics could result in different properties. These results suggest that this is an important aspect in engineering nanoparticles. The present technique enables the optimization of the properties of nano-microparticles through the tuning of the processing parameters, rather than by changing the chemical compositions. This feature would be a great advantage for tailoring particulate systems in cases where it is not desirable to use additives (e.g., food systems and cosmetics) or where chemical formulations cannot be tuned on site (e.g., pharmaceutics and medical cosmetics). The present approach potentially gives a novel processing strategy for engineering core–shell nanoparticles.

4. Conclusions

In this work, a freezing process was applied to the kinetics control of gelatin–acacia complex coacervation for encapsulating emulsified oil droplets. The o/w emulsions stabilized by gelatin–acacia solutions were prepared, and the pH levels of the solutions were adjusted to the selected values with acetic acid. Clear phase separations (creaming) were confirmed in the emulsions with pH levels of 3.0 and 4.0, whereas the emulsions with pH levels higher than 4.7 were visibly stable at ambient temperature for up to 12–24 h. As a consequence of freezing, the cream layers were apparently confirmed in the freeze-thawed solutions. This could be partly because of polymer phase separation (complex coacervation) in the cryoconcentrated phase. It was confirmed by TEM observation that the oil droplets were encapsulated with polymeric membranes to form core–shell nano-microparticles (approximately 50–4000 nm) and accumulated in the cream layer. The membrane properties were found to be dependent on the cooling rate during freezing. When an emulsion with a pH of 4.7 was frozen, a cooling rate of −1.0 °C/min maximized the encapsulation yield, whereas a rate of −2.0 °C/min was effective in limiting the release rate of the ingredient through the shell membrane. On the other hand, in the emulsions with pH levels of 3.0 and 4.0, complex coacervation occurred before freezing. In these cases, freezing did not greatly alter the membrane properties but caused damage due to ice crystal formation. This study suggests that the formation of particulate systems could be highly associated with the kinetics of freezing, so the resultant properties of nano-microparticles could be tuned using a freezing operation.

References

[1] P.L. Madan, L.A. Luzzi, J.C. Price, Factors influencing microencapsulation of a waxy solid by complex coacervation, J. Pharm. Sci. 61 (1972) 1583–1586.
[2] H. Takenaka, Y. Kawashima, S.Y. Lin, Micromeritic properties of sulfamethoxazole microcapsules prepared by gelatin–acacia cacervation, J. Pharm. Sci. 69 (1980) 513–516.
[3] H. Jizomoto, E. Kanaoka, K. Sugita, K. Hirano, Gelatin–acacia microcapsules for trapping micro oil droplets containing lipophilic drugs and ready disintegration in the gastrointestinal tract, Pharm. Res. 10 (1993) 1115–1122.
[4] J.M. Irache, L. Bergougnoux, I. Ezpeleta, J. Gueguen, A.M. Orecchioni, Optimization and in vitro stability of legumin nanoparticles obtained by a coacervation method, Int. J. Pharm. 126 (1995) 103–109.
[5] G.F. Palmieri, S. Martell, D. Lauri, P. Wehrle, Gelatin–acacia complex coacervation as a method for ketoprofen microencapsulation, Drug Dev. Ind. Pharm. 22 (1996) 951–957.
[6] B.A. Heelan, O.I. Corrigan, Preparation and evaluation of microspheres prepared from whey protein isolate, J. Microencap. 15 (1998) 93–105.
[7] M. Kaloti, H.B. Bohidar, Kinetics of coacervation transition versus nanoparticle formation in chitosan–sodium tripolyphosphate solutions, Colloids Surf. B: Biointerfaces 81 (2010) 165–173.
[8] A.S. Prata, M.H.A. Zanin, M.I. Ré, C.R.F. Grosso, Release properties of chemical and enzymatic crosslinked gelatin-gum Arabic microparticles containing a fluorescent probe plus vetiver essential oil, Colloids Surf. B: Biointerfaces 67 (2008) 171–178.
[9] D.V. Mendanha, S.E.M. Ortiz, C.S. Favaro-Trindade, A. Mauri, E.S. Monterrey-Quintero, M. Thomazini, Microencapsulation of casein hydrolysate by complex coacervation with SPI/pectin, Food Res. Int. 42 (2009) 1099–1104.
[10] M.P. Nori, C.S. Favaro-Trindade, S.M. de Alencar, M. Thomazini, J.C. de Camargo Balieiro, C.J.C. Castillo, Microencapsulation of propolis extract by complex coacervation, LWT – Food Sci. Technol. 44 (2011) 429–435.
[11] J. Xiao, H. Yu, J. Yang, Microencapsulation of sweet orange oil by complex coacervation with soybean protein isolate/gum Arabic, Food Chem. 125 (2011) 1267–1272.
[12] C. Schmitt, S.L. Turgeon, Protein/polysaccharide complexes and coacervates in food systems, Adv. Colloid Interface Sci. 167 (2011) 63–70.
[13] F. Weinbreck, M. Minor, C.G. de Kruif, Microencapsulation of oils using whey protein/gum Arabic coacervates, J. Microencapsul. 21 (2004) 667–679.
[14] A. Madene, M. Jacquot, J. Scher, S. Desobry, Flavour encapsulation and controlled release – a review, Int. J. Food Sci. Technol. 41 (2006) 1–21.
[15] J.G. Nairm, Coacervation-phase separation technology, Adv. Pharm. Sci. 7 (1995) 93–219.
[16] C.G. de Kruif, F. Weinbreck, R. de Vries, Complex coacervation of proteins and anionic polysaccharides, Curr. Opin. Colloid Interface Sci. 9 (2004) 340–349.
[17] D.J. Burgess, J.E. Carless, Microelectrophoretic studies of gelatin and acacia for the prediction of complexcoacervation, J. Colloid Interface Sci. 98 (1984) 1–8.
[18] K.S. Mayya, A. Bhattacharyya, J.F. Argillier, Micro-encapsulation by complex coacervation: influence of surfactant, Polym Int. 52 (2003) 644–647.
[19] G.L. Koh, I.G. Tucker, Characterization of sodium carboxymethylcellulose–gelatin complex coacervation by viscosity, turbidity and coacervate wet weight and volume measurements, J. Pharm. Pharmacol. 40 (1988) 233–236.
[20] W. Li, G. Wu, H. Chen, M. Wang, Preparation and characterization of gelatin/SDS/NaCMC microcapsules with compact wall structure by complex coacervation, Colloids Surf. A: Physicochem. Eng. Aspects 333 (2009) 133–137.
[21] J.C. Kim, H.Y. Lee, M.H. Kim, H.J. Lee, H.Y. Kang, S.M. Kim, Preparation and characterization of chitosan/gelatin microcapsules containing triclosan, Colloids Surf. B: Biointerfaces 52 (2006) 52–56.
[22] A.N. Gupta, H.B. Bohidar, V.K. Aswal, Surface patch binding induced intermolecular complexation and phase separation in aqueous solutions of similarly charged gelatin–chitosan molecules, J. Phys. Chem. B 111 (2007) 10137–10145.

[23] S. Boral, H.B. Bohidar, Effect of ionic strength on surface-selective patch binding-induced phase separation and coacervation in similarly charged gelatin–agar molecular systems, J. Phys. Chem. B 114 (2010) 12027–12035.
[24] G.R. Chilvers, V.J. Morris, Coacervation of gelatin–gellan gum mixtures and their use in microencapsulation, Carbohydr. Polym. 7 (1987) 111–120.
[25] J.N. McMullen, D.W. Newton, C.H. Becker, Pectin–gelatin complex coacervates I: determinants of microglobule size, morphology, and recovery as water-dispersible powders, J. Pharm. Sci. 71 (1982) 628–633.
[26] C. Thies, Microencapsulation of flavors by complex coacervation, in: J.M. Lakkis (Ed.), Encapsulation and Controlled Release Technologies in Food Systems, Blackwell Publishing Inc., Iowa, 2007, pp. 149–170.
[27] C. Remuñán-López, R. Bodmeier, Effect of formulation and process variables on the formation of chitosan–gelatin coacervates, Int. J. Pharm. 135 (1996) 63–72.
[28] W. Kurz, D.J. Fisher, Solidification Microstructure: Eutectic and Peritectic, in Fundamentals of Solidification, Trans Tech Publications, Switzerland, 1992, pp. 93–115.
[29] M.C. Heller, J.F. Carpenter, T.W. Randolph, Manipulation of lyophilisation-induced phase separation: implications for pharmaceutical proteins, Biotechnol. Prog. 13 (1997) 590–596.
[30] B. Bhatnagar, R.H. Bogner, M.J. Pikal, Protein stability during freezing: separation of stresses and mechanisms of protein stabilization, Pharm. Dev. Technol. 12 (2007) 505–523.
[31] Y.S. Gu, E.A. Decker, D.J. McClements, Application of multi-component biopolymer layers to improve the freeze-thawstability of oil-in-water emulsions: β-lactoglobulin–ι-carrageenan–gelatin, J. Food Eng. 80 (2007) 1246–1254.
[32] S. Muna, Y. Cho, E.A. Decker, D.J. McClements, Utilization of polysaccharide coatings to improve freeze–thaw and freeze–dry stability of protein-coated lipid droplets, J. Food Eng. 86 (2008) 508–518.
[33] K. Nakagawa, S. Surassmo, S.G. Min, M.J. Choi, Dispersibility of freeze-dried poly(epsilon-caprolactone) nanocapsules stabilized by gelatin and the effect of freezing, J. Food Eng. 102 (2011) 177–188.
[34] P. Bejrapha, S. Surassmo, M.J. Choi, K. Nakagawa, S.G. Min, Studies on the role of gelatin as a cryo- and lyo-protectant in the stability of capsicum oleoresin nanocapsules, J. Food Eng. 105 (2011) 320–331.
[35] K. Nakagawa, H. Nagao, S. Surassmo, S.G. Min, M.J. Choi, Stabilization of microcapsules by freeze-dried gelatin matrix: aqueous redispersibility and the ingredient activity, Dry Technol. 30 (2012) 416–424.
[36] R.W. Korsmeyer, R. Gurnya, E. Doelkera, P. Buria, N.A. Peppas, Mechanisms of solute release from porous hydrophilic polymers, Int. J. Pharm. 15 (1983) 25–35.
[37] P.L. Ritger, N.A. Peppas, A simple equation for description of soluterelease. II. Fickian and anomalous release from swellable devices, J. Control Release 5 (1987) 37–42.
[38] A. Tiwari, S. Bindal, H.B. Bohidar, Kinetics of protein–protein complex coacervation and biphasic release of salbutamol sulfate from coacervate matrix, Biomacromolecules 10 (2009) 184–189.
[39] F. Weinbreck, R.H. Tromp, C.G. de Kruif, Composition and structure of whey protein/gum Arabic coacervates, Biomacromolecules 5 (2004) 1437–1445.